Proceedings of ASME Turbo Expo 2011
GT2011
June 6-10, 2011, Vancouver, British Columbia, Canada

GT2011-46181

EFFECTS OF THERMAL TRANSIENTS ON CRACKED SHAFT VIBRATIONS

A. Vania **P. Pennacchi** **S. Chatterton**
Politecnico di Milano, Dept. of Mechanical Engineering
Via La Masa, 1, I-20156, Milano, Italy

ABSTRACT

Thermal transients can cause significant changes in the dynamic behavior of cracked rotors. The thermal expansions of the shafts cause changes of the distribution of stresses and strains, whose effects can give rise to the separation or the contact between portions of the surfaces of transverse cracks. This phenomenon can cause significant changes of the local flexural stiffness of the rotor, in the area close to the cracked section, and of the shaft lateral vibrations. However, this phenomenon must not be confused with the crack breathing, that is the periodic opening and closure of a transverse crack, caused by the machine weight, which occurs over a complete revolution of horizontal shafts. This paper is focused on the study of the effects of thermal transients on cracked shaft vibrations. With regard to this, the results obtained by the analysis of the experimental behavior of a cracked steam turbine are shown and discussed.

INTRODUCTION

The early detection of a crack propagation in the shafts of rotating machines, performed only by the analysis of vibration data, is very important to reduce the risk of a catastrophic damage. In fact, owing to the complex geometrical characteristics of the rotors, non destructive tests (e.g. UT) are often difficult to be performed. Moreover, they require long and costly outages. However, the effects caused by cracked shafts in the machine dynamic behavior are often rather small and masked by the symptoms of other common malfunctions. In general, the analysis of the shaft vibration gives a reliable identification of shaft cracks only when the severity of this fault is considerable.

Many model-based methods are available in literature to study the behavior of cracked shafts (1, 2, 3), however, many of these diagnostic techniques mainly emphasize the dynamic effects caused by the crack breathing phenomenon generated by the shaft weight giving a minor importance to the effects caused by the thermal transients that often affect the rotors.

In this paper, the experimental dynamic behavior of a cracked steam turbine in which a deep circumferential annular crack propagated, is shown. The description of this study has been integrated with the results of model-based investigations.

At first, the periodic breathing of the crack caused by the shaft weight has been studied. Then, a diagnostic method that allows simulating the changes of the turbine vibrations generated by the progressive closure of the crack caused by the machine heating has been developed. The successful results obtained by applying this technique to the case study are shown and discussed.

CASE STUDY

In this paper, the dynamic behavior of the steam turbine of a combined cycle power plant has been analyzed. The machine-train was composed of a 120 MW industrial gas turbine, a generator and a 50 MW steam turbine (ST). Figure 1 shows the steam turbine configuration and the support numbers. Load couplings were mounted between the two turbines and the opposite ends of the generator rotor. A clutch enabled the steam turbine to be connected to the generator in on-load condition.

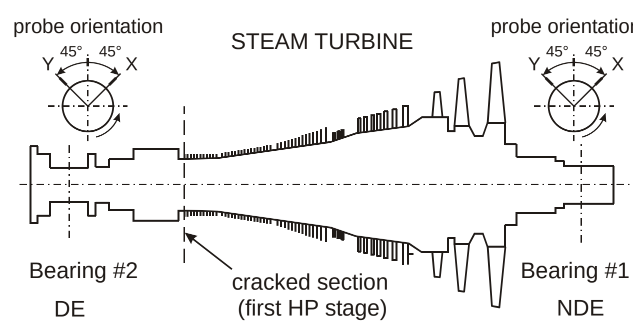

Figure 1. Steam turbine and bearing numbers.

The operating speed of the shaft-train was 3000 rpm. The ST shaft was mounted on two five-pad tilting pad journal bearings. Each support was equipped with a pair of XY proximity probes, mounted 90° degrees apart (Figure 1), that measured the shaft-to-support relative vibration. A pair of accelerometers, mounted in the same directions of the proximity probes, measured the support absolute vibration.

Crack characteristics

At the end of a long investigation performed after having detected the symptoms of a machine malfunction in the shaft vibrations, measured both in operating condition and during rotational speed transients, the steam turbine was removed from the shaft-train (4). Then, the blades of the first twenty-seven high-pressure (HP) stages were machined and removed since they could not be dismounted without destroying them.

A detailed final inspection of the rotor allowed finding a circumferential transverse crack in the shaft at the bottom of the bucket where the blades of the first HP stage were mounted.

This crack extended over the whole circumference while the average depth was nearly 50% of the nominal radius. Therefore, when the turbine was put out of service the area of the crack surface was extended to nearly 75% of the nominal cross-section (Figure 2 and Figure 3). The diagnostic strategy used to be confident that a transverse crack propagated in the turbine shaft, without having the opportunity to perform non-destructive tests, is shown in (4).

Transient vibrations of the cracked shaft

After a planned maintenance, during which only minor activities were carried out on the steam turbine, the unit was operated for six months with base load and partial loads without detecting any significant symptom of malfunction in the diagnostic analysis of vibration data and process parameters.

During this period nearly eighty start-ups were performed accordingly to the energy market demands while about 130 start-ups occurred in the previous ten years' life of this turbine. Owing to this, after the last planned maintenance the shaft was subjected to a considerable number of thermal transients that caused significant mechanical stresses in the rotor.

Then, during the first load rise performed at the end of a runup that occurred after a short outage, the amplitude of the 1X vibrations of the steam turbine reached considerable levels and showed a significant sensitivity to the machine thermal state. This dynamic behavior showed to be repetitive during three further attempts to operate the turbine in on-load condition carried out during the next three weeks. After having performed some basic inspections (4), which gave unsuccessful results, it was decided to restart the unit.

When the rotational speed reached 800 rpm it was maintained constant for about 70 minutes to stabilize the machine thermal expansions and limit some critical effects in the mechanical stresses caused by the turbine heating.

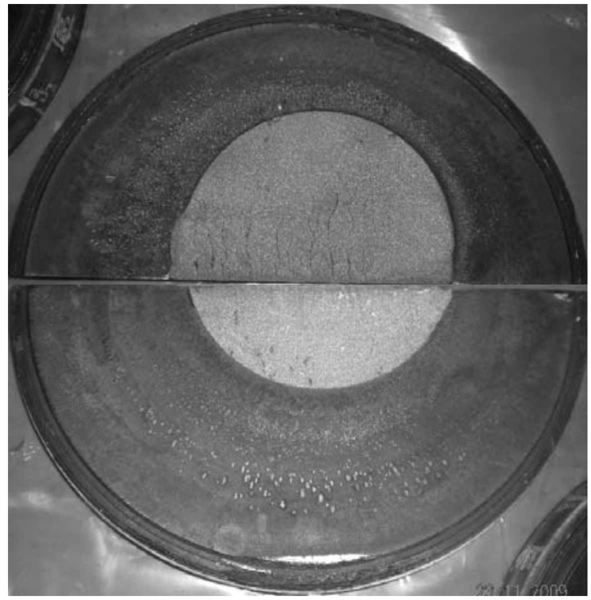

Figure 2. Cross-section of the cracked shaft.

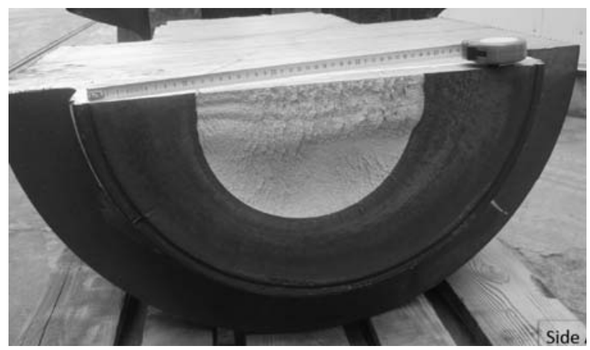

Figure 3. Cracked section of the steam turbine.

After this dwell, the shaft rotational speed was increased up to 3000 rpm. Figure 4 shows the Bode plot of the shaft-to-support 1X relative vibrations measured at the DE bearing #2 during the complete runup. The amplitude and phase curves show the presence of a flexural critical speed close to 1600 rpm.

When the rotational speed approached half this critical speed the amplitude of the 2X vibration measured at bearing #2 (Figure 5) showed a very small but evident increase. The level of these vibrations reached a peak at 785 rpm. This behavior was caused by the excitation of the shaft resonance, associated with the critical speed close to 1600 rpm, by means of the 2X dynamic forces generated at 785 rpm by the periodic closure of the crack, under the effect of weight, during a complete shaft revolution. In this case study these effects are rather limited owing to the particular shape of the crack.

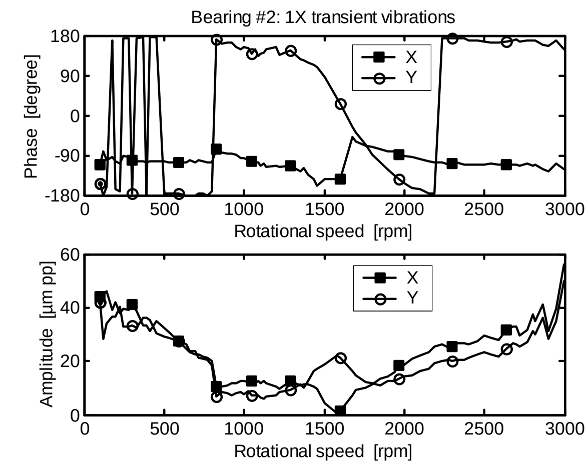

Figure 4. Bode plot of the 1X relative vibrations measured at bearing #2 during a runup.

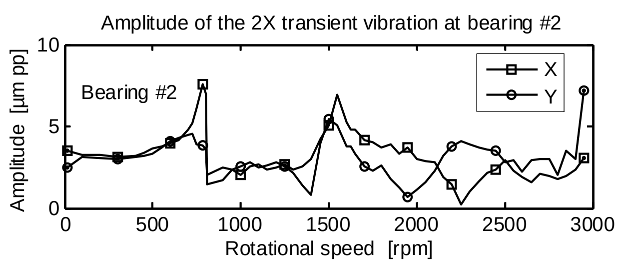

Figure 5. Amplitude of the 2X relative vibrations measured at bearing #2 during a runup.

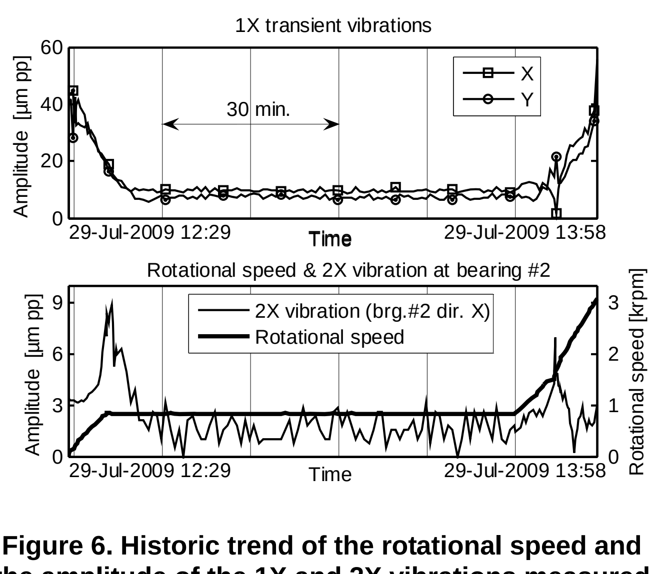

Figure 6. Historic trend of the rotational speed and the amplitude of the 1X and 2X vibrations measured at bearing #2 during a runup.

Figure 6 shows the historic trend of the amplitude of the 1X and 2X relative vibrations measured during the runup at bearing #2.

In the same figure, the historic trend of the turbine rotational speed is shown. The amplitude curves illustrated in Figure 6 show that the rotational speed pause performed at 800 rpm caused a progressive decrease of the amplitude both of 1X and 2X vibrations. This caused the sharp change of the 2X vibration level pointed out by the curves illustrated in Figure 5. This behavior can be explained as the consequence of the progressive closure of the crack caused by the turbine heating.

In fact, owing to the machine thermal transient, the temperature gradient generated in radial direction causes high negative axial strains, and compression stresses, in the outer part of the shaft, which tend to close the crack, as well as lower positive axial strains, and tensile stresses, in the inner part of the rotor.

At the end of the runup the amplitude of the 1X vibrations was sufficiently low at any measurement point. This indicates that the residual unbalance was rather small. Owing to the crack shape the levels of the 2X vibrations were very low and nearly constant during the complete runup: only in the speed ranges close to 785 rpm, 1600 rpm and 3000 rpm small increases of the 2X vector amplitude occurred.

Dynamic behavior in operating condition

Few minutes after reaching the operating speed a partial load rise was carried out, then the load was maintained constant at 10 MW for about 110 minutes. Figure 7 shows the historic trend of the 1X vector of the relative vibrations measured at bearings #1 and #2 during this time interval. It is possible to note that about five minutes after the beginning of the partial load rise these 1X vibrations show a smoothed peak that, at bearing #2, reached a maximum level of about 72 µm pp.

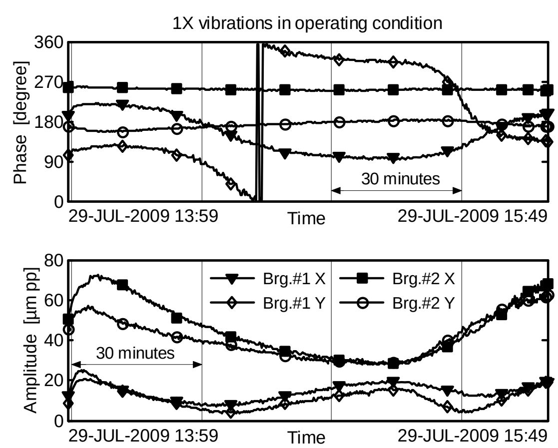

Figure 7. Historic trend of the 1X vibration at bearings #1 and #2 with a constant load of 10 MW.

Then, at each measurement point the amplitude of the turbine vibrations began to slowly decrease. After about seventy minutes, at bearing #2, the 1X vectors reached a minimum amplitude of 28 µm pp. In the end, these vibration levels began to increase with a constant trend and reached 70 μm pp after nearly thirty minutes. All these vibration changes occurred with a constant load and a constant steam temperature of 480°C. At bearing #2, located not so far from the first HP stage, the significant changes of the vibration amplitude were associated with unimportant changes of the 1X vector phase. Figure 8 shows the historic trend of the amplitude of the 2X relative vibrations measured at bearing #2 during the same on-load operating condition.

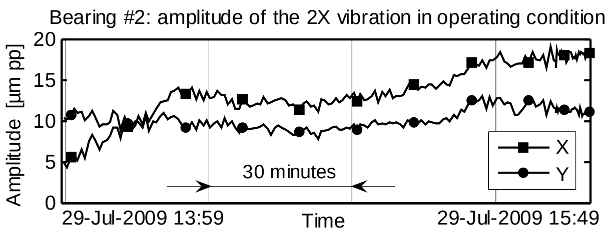

Figure 8. Historic trend of the 2X vibration at bearing #2 with a constant load of 10 MW.

The amplitude curves of the 2X harmonic component show unimportant changes over all the observation interval except for the measurement point oriented in the X direction at which the level of the 2X vibration was affected by an increase of about 5 μm pp in the initial and final parts of the on-load operating period reaching a maximum value of 18 μm pp.

The slow but continuous decrease of the amplitude of the 1X vibrations measured at bearing #2 in the initial part of the monitoring period carried out in on-load operating condition can be explained as a consequence of the shaft heating on the crack closure. The partial load rise up to 10 MW causes a thermal transient and a consequent temperature gradient in the shaft, in radial direction. In this thermal condition, the circumferential annular crack tends to close, independently on the rotor angular position. This phenomenon increases the flexural stiffness of the shaft and reduces the shaft bending as well as the amplitude of the 1X vibrations.

It is possible to suppose that about seventy minutes after the load rise beginning, the shaft temperature at the core equalizes that of the surface. These results are in accordance to those obtained by the turbine manufacturer. The decrease of the temperature gradient in radial direction nullifies the axial strains induced by the thermal effects, therefore the crack closure tends to be subjected only to the periodic changes, due to the weight, that occur during a complete shaft revolution. Owing to this, nearly eighty minutes after the beginning of the load rise, the amplitude of the 1X vibrations measured at bearing #2 changed their negative trend and began to increase.

Although the turbine thermal state significantly influenced the shaft dynamic behavior, the 2X vibrations showed only minor changes during the machine heating. This behavior was caused by the particular annular shape of the crack.

The crack breathing phenomenon caused by the gravity force during a complete revolution of the shaft has been studied by means of well known basic theories (1, 4, 5) that assume that the crack has plane surfaces and a very small thickness. For each shaft angular position the portion of the crack surfaces that should be ideally subjected to longitudinal tensile stresses has been evaluated by applying an iterative procedure. This portion of the crack is open. Moreover, in accordance with the previously mentioned assumptions, the portion of the facing surfaces of the crack subjected to compression stresses have been considered in contact. Then, the position of the neutral axis of the cracked section as well as of the area moment of inertia of this section, with respect to the principal axes, have been evaluated (Figure 9). Note that the maximum values of the inertia moments, $J_{x'}$ and $J_{y'}$, are associated with a shaft rotation of about 30°, for which the resistant area of the cracked shaft is nearly symmetrical with respect to the vertical axis.

Table 1 summarizes the main results of the order analysis of the periodic changes of the principal area moments of inertia of the cracked section caused by the breathing phenomenon. The harmonic content is dominated by the 1X order term while the other harmonic components are negligible. Therefore, also the amplitude of the 2X vibration of the shaft is not very high. This behavior is in accordance with the small local anisotropy caused by an annular crack that shows a nearly constant depth.

In the end, Figure 10 shows the effects of the opening and closing phenomenon of the crack for a limited number of significant angular positions of the shaft.

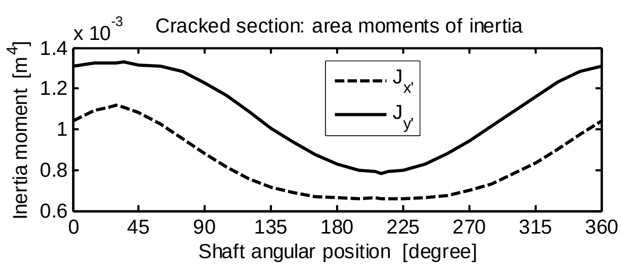

Figure 9. Changes of the area moments of inertia caused by the breathing phenomenon of the crack.

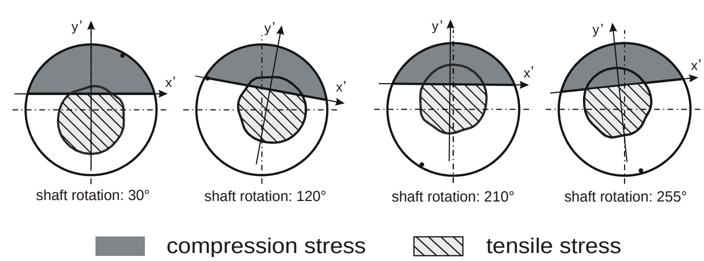

Figure 10. Breathing phenomenon of the crack caused by the shaft bending induced by the weight.

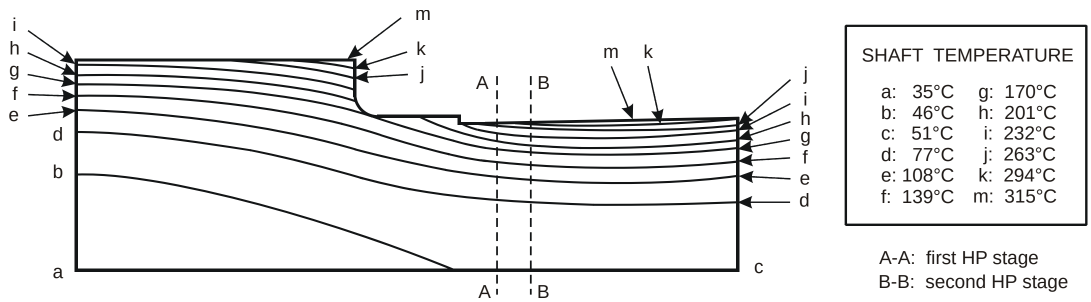

Figure 11. Temperature distribution in the turbine shaft evaluated twenty minutes after the beginning of the machine heating caused by a runup.

Table 1. Order analysis of the principal area moments of inertia of the cracked section evaluated over a complete revolution.

	PRINCIPAL INERTIA MOMENTS	
	$J_{x'}$	$J_{y'}$
Harmonic Order	[m^4]	[m^4]
Mean value	8.235×10^{-4}	1.075×10^{-3}
1X	2.158×10^{-4}	2.777×10^{-4}
2X	5.809×10^{-5}	1.546×10^{-5}
3X	9.427×10^{-6}	6.626×10^{-6}
4X	5.845×10^{-6}	5.069×10^{-6}

EFFECTS OF THE MACHINE HEATING

During the runups performed with the turbine in a cold thermal state, the shaft is subjected to a significant thermal transient. The blades of the first HP stages and the shaft surface are in contact with a steam flow whose temperature is 480°C. This generates a considerable temperature gradient in the shaft, in radial and axial direction. The evolution of the temperature distribution in the shaft, caused by the progressive heating, has been studied by the machine manufacturer by means of an accurate 3D Finite Element Model in which the turbine shaft and the blades of the first three HP stages have been considered. In this study the heat conduction phenomena in the rotor and the heat convection phenomena between the hot steam flow and the external surface of shaft and blades have been taken into account. As the results of this investigation are confidential, only a limited set of data is reported in this paper.

Figure 11 shows the theoretical temperature distribution in the shaft, evaluated in the axial and radial direction, twenty minutes after the beginning of the opening of the steam inlet valve. At the cross-section corresponding to the first HP stage, the temperature of the external surface is 315°C while that of the core is nearly 50°C. At the bottom of the blade bucket, where multiple initiations of the crack occurred, the temperature is 225°C. In the area close to the external surface of the shaft the temperature gradient is rather important.

These results, provided by an accurate FE model in which the most important thermal phenomena have been considered, have been used to tune an approximated model that is much simpler to be managed and that has allowed performing less time-consuming investigations. Nevertheless, as proven in the following, although this simple method is not rigorous, as it applicable only to a continuous cylinder, it has provided successful results that are in good accordance with the experimental evidences.

It is well known that in the case of a sufficiently long cylinder having a constant diameter, whose external surface is maintained at a constant temperature T_1, the radial distribution of the shaft temperature, evaluated at the time t, can be expressed as:

$$T(r) = T_1 - \left(T_1 - T_0\right) \sum_{n=1}^{\infty} \left[A_n \, J_0 \left(\beta_n \frac{r}{r_e} \right) e^{-\frac{\kappa \beta_n^2}{c \rho} \frac{t}{r_e^2}} \right] \tag{1}$$

where T_0 is the initial temperature of all the cylinder, r_e is the external radius of the shaft, κ is the coefficient of thermal conductibility, ρ is the shaft density, c is the specific heat and the terms A_n are given by:

$$A_n = \frac{2}{\beta_n J_1(\beta_n)} \tag{2}$$

The terms J_0 and J_1 are the Bessel functions of order zero and one, respectively, while β_n is the n-th solution of the Bessel function: $J_k(x) = 0$. The eq.(1) has been used to estimate the radial temperature distribution of a long equivalent cylinder whose radius, r_e, is equal to that corresponding to the bottom of the blade bucket of the first HP stage ($r_e = 250$ mm). In this case study, in accordance with the results shown in Figure 11, the temperature of the external surface of this equivalent cylinder has been maintained constant to 225°C while an initial temperature of 50°C has been assigned to whole the shaft.

Figure 12 shows the temperature distribution evaluated with eq.(1), in radial direction, after a time interval of 160 s. In the same figure, the temperature distribution in the real shaft, evaluated at a cross-section very close to the crack axial position by means of an accurate FEM (Figure 11), is shown. The external radius at the top of the blade bucket was $R = 274$ mm. The temperature of the external surface of the shaft has been assumed to be constant in this study.

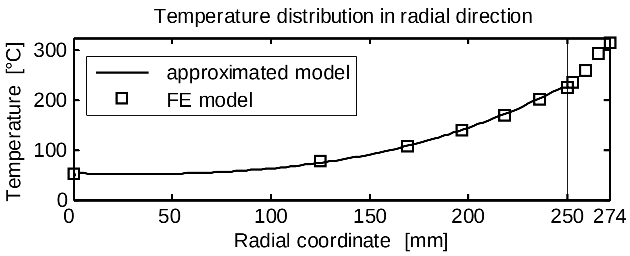

Figure 12. Temperature distribution evaluated in radial direction, in the cross-section corresponding to the 1st HP stage, 20 minutes after the beginning of the machine heating caused by a runup.

Given the short duration of the observation interval (160 s), this assumption is not too restrictive. For a radial coordinate ranging from 0 mm to 250 mm, the two curves illustrated in Figure 12 are very similar. Therefore, under the above mentioned assumptions, the simple model based on eq.(1) is able to provide a reliable estimate of the radial distribution of the shaft temperature, evaluated in the cracked cross-section, that occurs in the real machine twenty minutes after the beginning of the turbine heating.

According to thermoelasticity linear models, that are consistent with eq.(1), the stresses in axial, $\sigma(z)$, radial, $\sigma(r)$, and tangential, $\sigma(\theta)$, directions can be expressed as:

$$\sigma(z) = B\sum_{n=1}^{\infty} e^{-\frac{\kappa\beta_n^2}{c\rho}\frac{t}{r_e^2}}\left[\frac{1}{\beta_n^2}-\frac{1}{\beta_n^2}\frac{r}{r_e}\frac{J_1(\beta_n\ r/r_e)}{J_1(\beta_n)}\right]$$

$$\sigma(r) = B\sum_{n=1}^{\infty}\left\{e^{-\frac{\kappa\beta_n^2}{c\rho}\frac{t}{r_e^2}}\left[\frac{1}{\beta_n^2}+\frac{1}{\beta_n^2}\frac{r}{r_e}\frac{J_1(\beta_n\ r/r_e)}{J_1(\beta_n)}-\frac{J_0(\beta_n\ r/r_e)}{\beta_n\ J_0(\beta_n)}\right]\right\}$$

$$\sigma(\vartheta) = B\sum_{n=1}^{\infty} e^{-\frac{\kappa\beta_n^2}{c\rho}\frac{t}{r_e^2}}\left[\frac{2}{\beta_n^2}-\frac{J_0(\beta_n\ r/r_e)}{\beta_n\ J_1(\beta_n)}\right] \tag{3}$$

where the term B is given by:

$$B = \frac{2\,\alpha E(T_0 - T_1)}{1-\nu} \tag{4}$$

being α the coefficient of thermal expansion, E the Young's modulus and ν the Poisson's ratio. Figure 13 shows the distribution of the stresses, $\sigma(z)$, $\sigma(r)$ and $\sigma(\theta)$, evaluated in the healthy shaft twenty minutes after the beginning of the turbine heating. In the area of the cracked cross-section close to the turbine core, the shaft is subjected to tensile stresses, while in the area close to the external surface, compression stresses are generated by the machine heating. In this case study, the maximum value of these compression stresses is considerable (about -386 MPa). At a critical radial distance, R^*, of about 185 mm, the sign of the axial stress, $\sigma(z)$, changes.

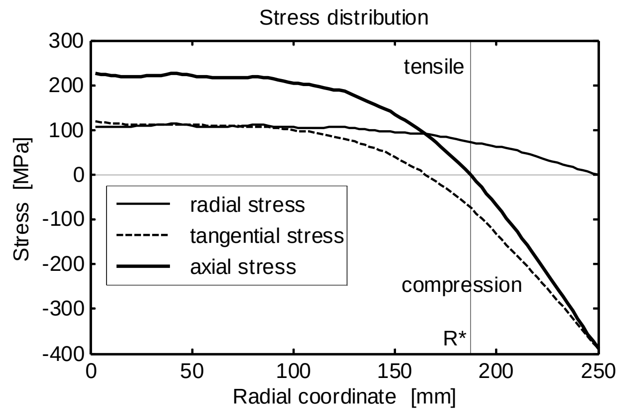

Figure 13. Stress distribution evaluated in radial, tangential and axial direction, at the cross-section corresponding to the 1st HP stage, 20 minutes after the beginning of the heating caused by a runup.

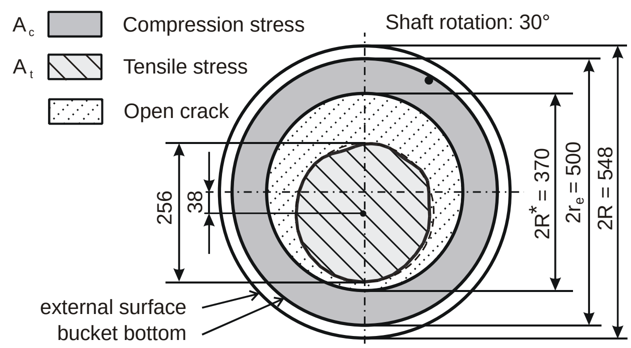

Figure 14. Crack closure caused by the turbine heating evaluated twenty minutes after the beginning of a runup: theoretical results.

The entire area of the cross-section subjected to compression stresses is contained in the region affected by the annular crack. Therefore, in case of plane facing surfaces of the crack, it is possible to suppose that in the area subjected to the compression stresses, the crack surfaces are in contact. Conversely, a portion of the cross-section ideally subjected to tensile stresses is contained in the area affected by the annular crack. In this case, as tensile stresses cannot be transmitted, an inner portion of the crack is open. Figure 14 shows the areas of the cracked cross-section of the shaft subjected to tensile and compression stresses, as well as the region of the crack where the surfaces are not in contact.

Although the temperature distribution is axial symmetric, the presence of the crack, of a part of the cracked surfaces that are not in contact and, in the end, the eccentricity of the residual section, cause a distortion of the nominal distribution of the stresses illustrated in Figure 13. Moreover, a more rigorous study should consider the additional stresses generated at the tip of the crack as well as the stresses caused by turbine weight and centrifugal forces. However, in the area close to the external surface of the shaft as well as in that close to the core, the effects caused by the machine heating give a dominant contribution to the mechanical stresses. Therefore, in the following, the periodic breathing phenomenon of the crack caused by the shaft weight and by all the other phenomena that do not depend on the shaft heating have been neglected.

The considerable compression stresses generated by the turbine heating at the highest radial distance cause a progressive closure of the annular crack. Contrarily to the crack breathing phenomenon induced by the shaft weight, this crack closure is not periodic as it is weakly influenced by shaft angular position. The radius $R^*(t)$ at which the sign of the axial stresses changes, that is the maximum radial distance at which the crack is open, depends on time t and temperature $T(r,t)$. Given a radius R^*, the principal area moments of inertia, $J_{x'}$ and $J_{y'}$, of the cracked section, can be evaluated. These parameters influence the local flexural stiffness of the shaft and then the turbine dynamic behavior. Owing to the particular annular shape of the crack, the inertia moments $J_{x'}$ and $J_{y'}$ are rather similar. Therefore, the mean value, J_m, of these inertia moments can be considered to obtain a reliable estimate of the local flexural stiffness of the shaft. Then, the equivalent radius r_{eq} of a circular section having the same area moment of inertia, J_m, can be evaluated.

The turbine vibrations measured during the first cold runup, in the rotational speed range from 150 rpm to 800 rpm, have been simulated by means of a model-based method developed in the past by the Dept. of Mechanical Engineering of the Politecnico di Milano (6, 7, 8). Figure 15 shows the beam Finite Element model of the turbine shaft. Moreover, the mechanical characteristics of the foundation structure and the speed dependent stiffness and damping coefficients of the oil-film journal bearings, have been included in the machine model.

The original diameter of the two beam finite elements located near the cracked section was suitably modified during this study to simulate the changes of the local flexural stiffness caused by the crack closure generated by the turbine thermal transients. As the experimental vibration data are available only about eight minutes after the initial partial opening of the steam inlet valve, a delay must be considered to correlate the turbine dynamic behavior to the shaft heating and the consequent crack closure.

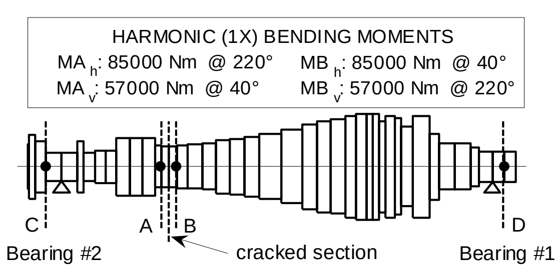

Figure 15. Finite element model of the turbine shaft.

Given a value of the radius $R^*(t)$ at which the sign of the axial stress evaluated in the cracked section changes, the area A_c of the cross-section in which the crack surfaces are in contact, can be evaluated. In this section, during the turbine heating, the compression stresses act only in the annular area A_c, while the residual section A_t of the shaft is subjected only to tensile stresses (Figure 14). Let us denote A_g the global area composed of A_c and A_t. The coordinates of the centre of the area A_g and the principal area moments of inertia, can be evaluated. Then, the equivalent radius r_{eq} of a circular section having the same mean inertia moment J_m can be determined.

Two pairs of opposite harmonic bending moments, whose frequency is associated with the rotational frequency, have been applied to the shaft, in the horizontal and vertical plane, in the cross-sections A and B (Figure 15). The magnitude and phase of these bending moments that allows simulating the 1X vibrations measured at 150 rpm at bearings #1 and #2 have been estimated. In the following, magnitude, phase and axial position of these two pairs of bending moments have not been modified. The experimental data illustrated in the upper diagram of Figure 6 show that during the first 12 minutes of the runup the levels of the 1X vibrations measured at bearing #2 significantly decreased, from 40 μm pp to 10 μm pp, with the same rate during the initial speed ramp up to 800 rpm and during the subsequent speed dwell. This indicates that the vibrations were weakly affected by the rotational speed while they were significantly influenced by the turbine thermal state.

In the above described investigation an estimate of the radius $R^*(t)$, twenty minutes after the beginning of the shaft heating, has been obtained. In this thermal state, the significant closure of the crack caused an increase of the equivalent radius r_{eq} of the two beam elements included in the turbine model in close to the cracked section. Therefore, the amplitudes of the vibrations evaluated at 800 rpm, without changing the system excitations, is significantly lower than those obtained at 150 rpm. Moreover, these results proved to be in good accordance with the experimental evidences.

Then, a model-based iterative procedure has been applied to simulate the shaft vibrations measured during the first twelve minutes of the runup, starting from the time at which the rotational speed reached 150 rpm.

For a given value of the radius $R^*(t)$ the equivalent radius $r_{eq}(t)$ of the two beam elements included in the turbine model close to the cracked section has been evaluated. Then, for a given rotational speed, the turbine vibrations caused by the excitations reported in Figure 15 have been evaluated. If these predicted vibrations differed too much from the corresponding experimental data the computation of the turbine response has been repeated considering a different value of the rotational speed. The curves of the radii $R^*(t)$ and $r_{eq}(t)$, evaluated in the above mentioned time interval, are plotted in the upper diagram of Figure 16, while the corresponding trend of the turbine rotational speed is illustrated in the lower diagram. As the time history of the speed ramp up to 800 rpm was known (Figures 6,

16) it has been possible to correlate the changes of the radii R^* and r_{eq} to the time t.

In the Bode plot illustrated in Figure 17, the 1X vibrations evaluated at bearings #1 (NDE) and #2 (DE), in the X direction, are compared to the corresponding experimental data.

Although the 1X vibration levels measured at the two bearings during the runup are very different, the accordance between predicted and experimental vibrations is rather good. Moreover, the changes of the radii R^* and r_{eq}, over the entire observation period, are rather regular. This basic requirement for parameters that are affected by thermal phenomena allows supposing that the reliability of these results, obtained by means of an approximated method, is anyway satisfactory.

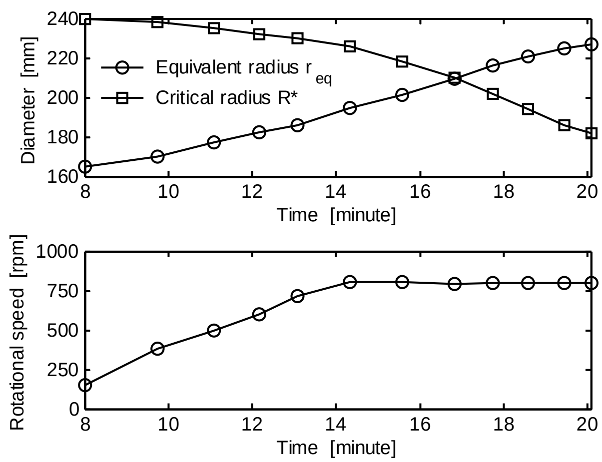

Figure 16. Historic trend of the crack closure caused by the turbine heating induced by a runup.

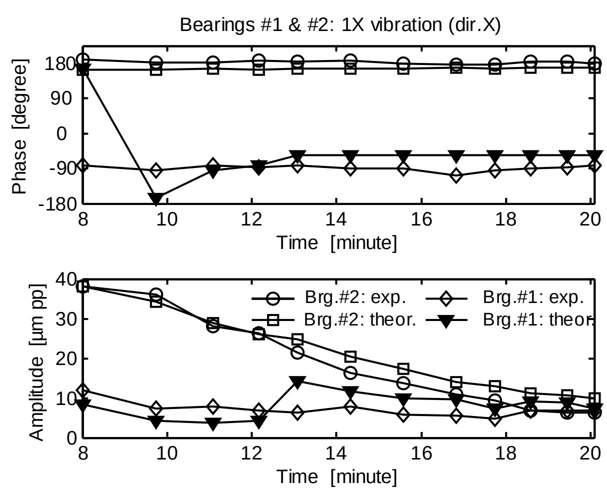

Figure 17. Historic trend of the 1X vibrations of the cracked shaft during the turbine heating: comparison between experimental data and numerical results.

CONCLUSION

The dynamic behavior of the cracked shaft of steam turbine has been studied in the paper. Owing to the unusual annular shape of the crack the amplitude of the 2X and 3X vibrations was rather small, although the crack depth was considerable. Conversely, the turbine 1X vibrations showed a significant sensitivity to the machine thermal transients as they caused a progressive closure, or opening, of the crack.

The periodic breathing phenomenon of the crack, evaluated over a complete shaft revolution, has been investigated with a model-based method. The results of this study have explained the reasons for the low levels of the 2X vibration of the shaft.

A limited set of data concerning the temperature distribution of the rotor, evaluated by the machine manufacturer in radial and axial direction by means of an accurate 3D FEM, allowed tuning a simple thermoelasticity model by means of which the progressive crack closure, caused by the turbine heating that occur during the runup and the following load rise, has been estimated.

Although a simple approximated method, based on a continuous cylinder, was used to study the heat transfer and the mechanical stresses in the cracked shaft, the results provided by this not rigorous approach allowed evaluating a satisfactory estimate of the changes of the shaft flexural stiffness that occurred during the turbine heating. The results provided by this investigation have been used to simulate the considerable changes that affected the 1X vibrations of the shaft experienced during the runups. The successful results that have been obtained are shown and discussed.

REFERENCES

1. Bachschmid N., Pennacchi P., Tanzi E., *Cracked rotors*, Springer, Berlin, Germany, (2010).
2. Darpe A.K., Gupta K., Chawla A., Couple bending longitudinal and torsional vibrations of a cracked rotor, Journal of Sound and Vibration, 269 (1-2), (2004), pp. 33-60.
3. Wu X., Friswell M.I., Sawicki J.T., *Finite element analysis of coupled lateral and torsional vibrations of a rotor with multiple cracks*, Proc. of ASME Turbo Expo Gas Turbine Technology: Focus for the Future, 2005, June, Vol. 4, pp. 841-850.
4. Vania A., Pennacchi P., *Shaft crack detection in a steam turbine: experimental evidences and model-based investigations*, Proc. of ISMA 2010, Int. Conf. on Noise and Vibration Engineering, Sept. 2010, Leuven, Belgium.
5. Papadopulos C.A., *Some comments on the calculation of the local flexibility of cracked shafts*, Journal of Sound and Vibration, 278 (4-5), 82004), pp. 1205-1211.
6. Bachschmid N., Pennacchi P., Vania A., *Identification of multiple faults in rotor systems*, (2002), Journal of Sound and Vibration, 254, No.2, pp.327-366.
7. Lalanne M., Ferraris G., *Rotordynamics Predictions in Engineering*, (1998), John Wiley & Sons Inc., Chichester, England.
8. Adams M., *Rotating machinery vibration*, (2001), Marcel Dekker Inc., New York, N.Y., USA.

